Journal of Hazardous Materials 219–220 (2012) 203–212

Contents lists available at SciVerse ScienceDirect

Journal of Hazardous Materials

journal homepage: www.elsevier.com/locate/jhazmat

Comparison of cytotoxic and inflammatory responses of pristine and functionalized multi-walled carbon nanotubes in RAW 264.7 mouse macrophages

Ting Zhang[a,b], Meng Tang[a,b,*], Lu Kong[a,b], Han Li[c], Tao Zhang[c], Shanshan Zhang[a,b], Yuying Xue[a,b], Yuepu Pu[a,b,**]

[a] Key Laboratory of Environmental Medicine Engineering, Ministry of Education, School of Public Health, Southeast University, Nanjing 210009, China
[b] Jiangsu Key Laboratory for Biomaterials and Devices, Southeast University, Nanjing 210009, China
[c] College of Engineering and Applied Sciences, Nanjing University, Nanjing 210093, China

ARTICLE INFO

Article history:
Received 15 December 2011
Received in revised form 2 March 2012
Accepted 29 March 2012
Available online 5 April 2012

Keywords:
MWCNTs
Cytotoxicity
Inflammation
Functionalized nanotubes
Macrophages

ABSTRACT

The increased application of carbon nanotubes (CNTs) has raised the level of public concern regarding possible toxicities. Using *in vitro* cellular assays, we were able to assess the immunotoxicity of pristine multi-wall carbon nanotubes (MWCNTs) and their derivatives, covalently functionalized with carboxyl (COOH) or polyethylene glycol (PEG), in rodent macrophage cells. Moreover, special focus was placed on the role of surface modification and nanotubes aggregation on toxicity. Results showed that pristine MWCNTs reduce cell viability compared with functionalized MWCNTs in RAW 264.7 macrophages when incubated at concentrations of 25, 50, 100, 200, 400, and 800 μg/mL. However, in addition to causing cytotoxicity, functionalized MWCNTs induce serious inflammatory responses, as indicated by the production of inflammatory cytokines including TNF-α, IL-1β and IL-6 at various MWCNTs concentrations (25, 50, 100, and 200 μg/mL). Particle surface modification and dispersion status in biological medium were key factors in determining cytotoxicity. These findings imply that MWCNTs-induced inflammatory responses in macrophages may be associated with surface modification and aggregation of MWCNTs, which is reflected by alteration of inflammatory cytokine expression.

1. Introduction

Carbon nanotubes (CNTs), including single- and multi-walled carbon nanotubes (SWCNTs and MWCNTs), vary significantly in size (1–20 nm width, and several hundreds of microns in length), strength, and surface chemistry [1]. CNTs have promising applications in electronics, aerospace, and in biology and medicine, where modified CNTs can serve as vaccine vehicles, protein transporters, and biosensors [2]. It is thought that widespread use of CNTs will lead to significantly increased occupational and public exposure [3] and they have already posed emerging health concerns [4,5]. Notably, their high length-to-width aspect ratio, reactive surface chemistry, and/or poor solubility raise concerns associated with previous occupational and public exposure, such as that associated with asbestos, which could be linked to a frustrated phagocytosis mechanism. Given this background, the generation of toxicity data, including exploration of the mechanisms by which CNTs might be absorbed, are urgently needed.

Many papers have been published on the potential health effects of CNTs, but they often describe conflicting results. For example, some studies showed that CNTs decrease cell viability [3,6] and up-regulate genes associated with inflammation and apoptosis [3,7–9]. However, others have shown minimal or no decrease in cell viability [10]. Therefore, existing data present significant complexity for accessing toxicity. A more recent focus on the physicochemical properties of CNTs has influenced the

Abbreviations: CNTs, carbon nanotubes; SWCNTs, single-walled carbon nanotubes; MWCNTs, multi-walled carbon nanotubes; COOH, carboxylate; PEG, polyethylene glycol; LDH, lactate dehydrogenase; FITR, fourier transform infrared spectroscopy; XPS, X-ray photoelectron spectroscopy; TGA, thermogravimetric analysis; ICP-MS, inductively coupled plasma mass spectrometry; TEM, transmission electron microscopy; DMEM, Dulbecco's minimum essential Eagle's medium; CCK-8, cell counting kit-8; ELISA, enzyme-linked immunosorbent assay; NED, *N*-(1-naphthyl)-ethylenediamine; GAPDH, glyceraldehyde 3-phosphate dehydrogenase; TNF-α, tumor necrosis factor-alpha; IL-1β, interleukin-1beta; IL-6, interleukin-6; NO, nitric oxide; iNOS, inducible nitric oxide synthase; CV, coefficient of variation; UV–VIS, ultraviolet and visible; OD, optical density; PBS, phosphate buffer solution.

* Corresponding author at: Key Laboratory of Environmental Medicine Engineering, Ministry of Education, School of Public Health, Southeast University, Nanjing 210009, China. Tel.: +86 025 83272564.
** Corresponding author at: Key Laboratory of Environmental Medicine Engineering, Ministry of Education, School of Public Health, Southeast University, Nanjing 210009, China. Tel.: +86 025 83794996, fax: +86 025 83783428.
E-mail addresses: tm@seu.edu.cn (M. Tang), yppu@seu.edu.cn (Y. Pu).

0304-3894/$ – see front matter © 2012 Elsevier B.V. All rights reserved.
http://dx.doi.org/10.1016/j.jhazmat.2012.03.079

interpretation of CNTs toxicity studies and the impacts that their physicochemical properties have on human health. Moreover, the omission of physicochemical characterization data complicates efforts to compare toxicity results between studies. First, toxicity and reactivity of CNTs depend on the characteristics of the specific type of material tested, surface area, and the tendency to agglomerate and disperse in media [4,11]. Second, the synthetic methods used produce impurities and leave metal catalyst residue, as does the purification processes involved [12]. Third, CNTs toxicity effects can also be modified by chemical functionalization [13]. Given the expense and complexity of assessing toxicity for each possible CNTs sample modification, general correlations between cytotoxicity and physicochemical properties of nanotubes is fundamental to low-risk commercial applications. These correlations will require simultaneous material characterization and standardized toxicity assays. Carefully documented and well-defined studies will also inform a mechanistic understanding of nanomaterial toxicity.

In this work, murine macrophage RAW264.7 cells were used to explore different toxicological responses of MWCNTs with various well-characterized CNTs. Macrophages are frequently used in primary toxicity studies since they offer a highly efficient defense system that can filter and clear particulate matter. Owing to their crucial role in processing particulate matter inhaled into the body, macrophages are considered suitable sensors for analyzing such potential adverse effects. Moreover, macrophages are potent producers of immune mediators including cytokines and chemokines, which participate in antigen presentation. Because of their importance in the immune system, numerous studies have addressed the effects of nanoparticles on macrophages both in cell culture system and *in vivo* [14]. However, to determine the link between toxicity and material property, it is necessary to perform a comparative study using CNTs libraries that have been well characterized with one or several key material properties.

The present study focused on toxicity effects that incorporate rational physical or chemical modifications to elucidate a mechanistic understanding of MWCNTs toxicity *in vitro*. We synthesized carboxylate (COOH) and polyethylene glycol (PEG) functionalized MWCNTs, and evaluated the immunotoxicological response after comparing the in-house synthesized and laboratory-made functionalized MWCNTs (MWCNTs-COOH and MWCNTs-PEG) with commercial MWCNTs (pristine MWCNTs). Physicochemical properties of the MWCNTs were carefully characterized and their cytotoxicity was evaluated in parallel by two classical methods for assessing changes in cell metabolism: (WST-8 assay) and membrane integrity (LDH assay). Furthermore, we assayed cytokine secretion to assess the inflammatory responses of macrophages to MWCNTs. Key factors leading to dispersion and quantitative cellular uptake of MWCNTs have been evaluated from the point of view of bioavailability and toxicity hierarchy. Careful correlation between physicochemical properties and cytotoxic observations will provide valuable predictive value, and inform mechanistic pathways of MWCNTs toxicity in macrophages.

2. Materials and methods

2.1. Cell culture and materials

The RAW 264.7 murine macrophage cell line was purchased from the Cell Culture Center of the Chinese Academy of Medical Sciences (Shanghai, China) and grown in Dulbecco's modified Eagle's medium (DMEM) supplemented with 10% fetal bovine serum (FBS). MWCNTs (diameter: 10–20 nm, length: 5–15 μm) were purchased from Shenzhen Nanotech Port Co. Ltd (Shenzhen, China). The hydrophilic derivatives of MWCNTs (MWCNTs-COOH, MWCNTs-PEG) were synthesized as previously described [15]. The samples (pristine MWCNTs, MWCNTs-COOH, MWCNTs-PEG) were characterized by Malvern Instruments Zetasizer Nano ZS90 (Worcestershire WR, UK), fourier transform infrared spectroscopy (FTIR, Perkin Elmer, Waltham, MA, USA), X-ray photoelectron spectroscopy (XPS, Thermo Scientific K-Alpha, USA), and validated with thermogravimetric analysis (PE Pyris1 TGE, Perkin-Elmer, USA), inductively coupled plasma mass spectrometry (ICP-MS, J-A1100, Jarrell-Ash, MA, USA), and transmission electron microscopy (TEM, JEM-2100, JEOL Ltd., Tokyo, Japan).

2.2. Cell viability assay

Cell viability was evaluated using the WST-8 Cell Counting kit (Keygen Biotech Company, Nanjing, China). Cells (5×10^4/mL) were cultured in 96-well plates and exposed to three different MWCNTs at six different concentrations (25, 50, 100, 200, 400 and 800 μg/mL) for 24 h. The cells alone with the same medium were used as negative controls. After 24 h incubation, the supernatant was transferred to 96-well plates. Plates were read with a Dynex MRX microplate reader (Dynex Technologies Inc., Chantilly, VA, USA) by measuring the optical density (OD) at 450 nm.

2.3. Measurement of membrane integrity using lactate dehydrogenase (LDH) assay

Cells (1×10^5/mL) were cultured in 24-well plates and exposed to pristine, –COOH, and –PEG MWCNTs, each at four concentrations (25, 50, 100, and 200 μg/mL), which are the same concentrations used in the assays described below. After incubating for 24 h, LDH activity was determined using an LDH assay kit (Jiancheng Bioengineering, Nanjing, China) according to the manufacturer's instructions.

2.4. Measurement of nitrite (NO)

Cells (1×10^5/mL) were cultured in 24-well plates and exposed to pristine, –COOH, and –PEG MWCNTs, each at four concentrations (25, 50, 100, and 200 μg/mL). After incubating for 24 h, nitric oxide synthesis was determined by assaying the culture medium for nitric oxide using the Griess reaction [16].

2.5. Real-time quantitative RT-PCR analysis

Cells (5×10^5/mL) were cultured in 6-well plates and exposed to pristine, –COOH, and –PEG MWCNTs, each at four concentrations (25, 50, 100, and 200 μg/mL) for 24 h. The culture medium was collected for antibody arrays (see below). Total RNA was extracted using the Trizol protocol (Invitrogen, Carlsbad, CA, USA). cDNA was synthesized from total RNA using Super Script III Reverse Transcriptase (Invitrogen). Real-time quantitative RT-PCR analysis was performed with an automated sequence detection system (ABI Prism 7300, Tokyo, Japan). Expression of mouse genes GAPDH, TNF-α, IL-1β, IL-6 and iNOS was analyzed using SYBR Green Premix Ex Taq II (TOYOBO, Osaka, Japan). Primers were designed using Primer Express Software according to guidelines (Table 1). The real-time PCR data were analyzed using the $2^{-\Delta\Delta CT}$ relative quantitation method, using the manufacturer's standards of GAPDH [17,18].

2.6. ELISA assay

Secretion of mouse IL-1β, TNF-α, and IL-6 was measured by ELISA using the "Ready-Set-Go" kit from eBioscience (San Diego, CA, USA). Media from three separate wells of RAW264.7 cells was assayed after treatment with MWCNTs for 24 h and absorbance measured at 450 nm.

Table 1
Primer sequences of inflammation-related genes used in this study.

Parameters	Primer sequences (5′ → 3′)
IL-1β	Reverse: TGTCCTCATCCTGGAAGGTC
	Forward: TGTGAAATGCCACCTTTTGA
IL-6	Reverse: TAAGCCTCCGACTTGTGAAGTGGT
	Forward: ATCCAGTTGCCTTCTTGGGACTGA
TNF-α	Reverse: CACTTGGTGGTTTGCTACGA
	Forward: CCACCACGCTCTTCTGTCTA
iNOS	Reverse: GCTCATGCGGCCTCCTTT
	Forward: CCTGGTACGGGCATTGCT
GAPDH	Reverse: ACAGCTTTCCAGAGGGGCCATC
	Forward: TTGTCAGCAATGCATCCTGCAC

2.7. Assessment of MWCNTs dispersion in cell culture medium

2.7.1. Characterization of MWCNTs suspension stability index

A kinetic analysis of suspension stability was performed as previously described [19]. Typically, 2 mL of the MWCNTs suspension (25, 50, 100, and 200 μg/mL) was prepared with DMEM and absorbance readings taken at 1 h time intervals for 24 h. The value at 0 h was designated A_0. For every aliquot, the absorbance of the aqueous layer was measured again (A_1), and the suspension stability index (%) was calculated as follows:

$$\text{Suspension stability index} = \frac{A_1}{A_0} \times 100\%$$

2.7.2. Visualization MWCNTs dispersion by light microscopy

A stock concentration (100 μg/mL) of pristine, –COOH and –PEG MWCNTs was prepared in DMEM. The MWCNTs suspensions were added to cell mixtures. Following a 24 h incubation, cell cultures were examined by phase contrast light microscopy (Olympus CX 41, Tokyo, Japan).

2.8. Cellular uptake of MWCNTs

2.8.1. Quantitative measurement of MWCNTs uptake by cells

Quantitative measurement of MWCNTs uptake was performed as previously described [20]. In brief, the MWCNTs stock suspension was diluted with cell lysis solution and the OD measured at 640 nm, followed by quantitation of MWCNTs. Cells were cultured in 6-well plates and exposed to 25 μg/mL MWCNTs for 2, 4, 6, 8, 12 and 24 h, washed with PBS and lysed with 0.4 mL of 0.2 mol/L NaOH solution for 3 h. Dimethyl sulfoxide (0.2 mL) was added to the lysate until MWCNTs were well dispersed in the lysate. A 250 μL sample was transferred to a 96-well plate and the OD at 640 nm was measured.

2.8.2. Transmission electron microscopy

After incubation with 200 μg/mL of MWCNTs for 24 h, RAW264.7 cells were fixed in 2.5% glutaraldehyde in 0.1 M phosphate buffer for 1 h, post-fixed in 1% OsO_4 in 0.1 M phosphate buffer for 1 h, dehydrated in ascending grades of ethanol and subsequently embedded in epoxy resin. The prepared ultra-thin sections (40 nm) were contrasted with 0.3% lead citrate and imaged with a transmission electron microscopy (JEM-1010, JEOL Ltd., Tokyo, Japan) at 80 kV.

2.9. Statistical analysis

All experiments were repeated at least three times. Data are presented as the mean ± standard deviation for the indicated number of independently performed experiments. Student's *t*-test was used for the determination of statistical significance with $p < 0.05$ being considered significant.

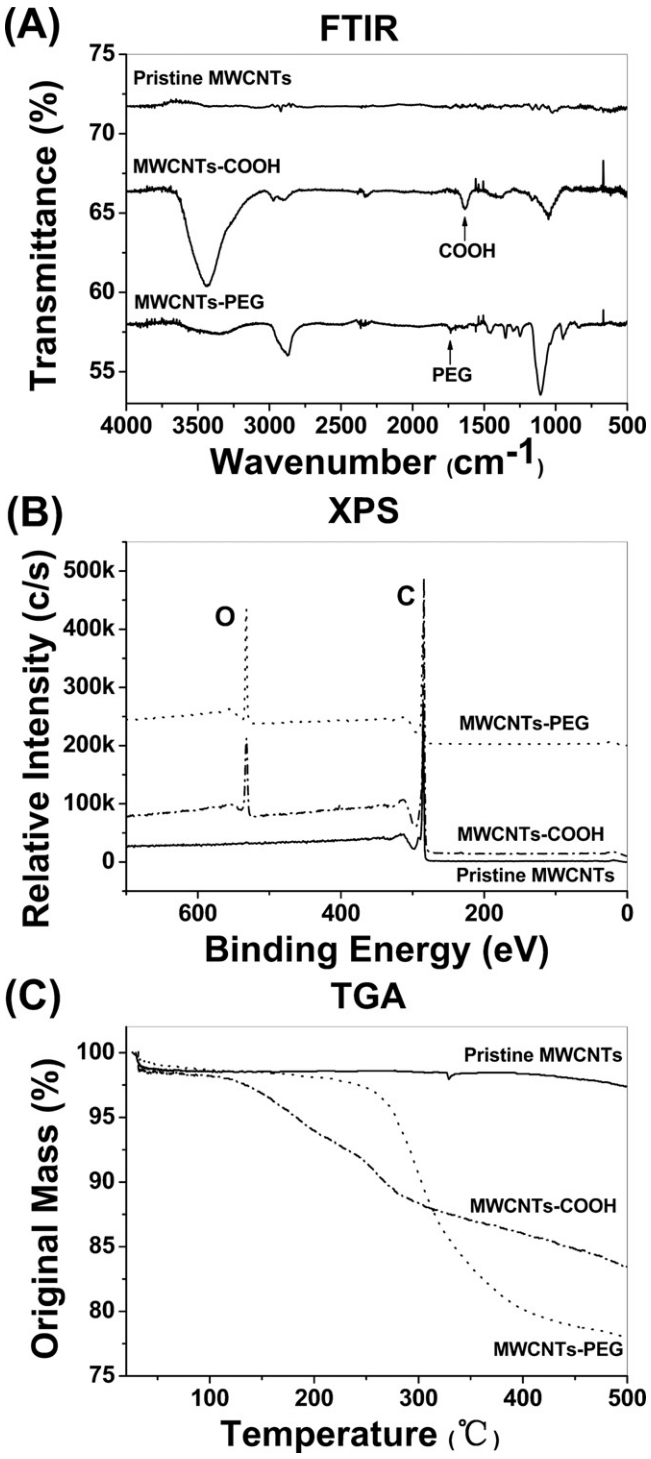

Fig. 1. Characterization of pristine MWCNTs and MWCNTs functionalized with carboxyl groups and polyethylene glycol. (A) FTIR spectra of MWCNTs in reflectance mode; (B) C1s spectrum of MWCNTs, analyzed with X-ray photoelectron spectroscopy; and (C) TGA curves of MWCNTs in nitrogen atmosphere.

3. Results

3.1. Characterization of MWCNTs

Microstructural characterization of the MWCNTs investigated in this study is summarized in Table 2, and Figs. 1 and 2. The zeta potentials indicated a negative absolute charge in all MWCNTs (Table 2). Data on pristine MWCNTs indicated the presence of

Table 2
Physicochemical characterization of the MWCNTs.

	Pristine MWCNTs	MWCNTs-COOH	MWCNTs-PEG
Length (μm)	~5 to 15	~5 to 15	~5 to 15
Diameter (nm)	~10 to 20	~10 to 20	~10 to 20
Zeta potential (mV in H_2O)	−34.5	−14.6	−9.8
Zeta potential (mV in 10% FBS DMEM)	−12.1	−11.7	−10.0
Purity (%)	98.9429	98.8456	99.0226
Impurities (wt%)	0.0767 Ni, 0.0174 Fe	0.1180 Ni, 0.0487 Fe	0.0585 Ni, 0.0104 Fe

Fe and Ni impurities at concentrations of 0.02% and 0.08%, respectively. Similarly, lower metal concentrations were found in the functionalized nanotubes. For each of the three MWCNTs, the Fe and Ni content were 0.01–0.05% and 0.06–0.12%, respectively. Thus, the remarkably similar metal content indicated low levels of impurities.

3.1.1. FT-IR spectroscopy

Fig. 1A shows the FTIR spectra of pristine and functionalized MWCNTs. For the former, the FTIR spectra exhibited a straight line and an absorbance peak was not assigned, indicating no surface modification. For the MWCNTs-COOH spectra, an absorption peak at 1600 cm^{-1} could be assigned to the COOH group and a peak at 3300 cm^{-1} could be assigned to the OH group. These peaks are indicative of successful COOH modification.

For the MWCNTs-PEG spectra, the 2920 cm^{-1} peak could be assigned to the methylene groups and the 1100 cm^{-1} peak to the C—O—C vibration. The absorbance bands at 1570, 1450, 1400 and 1240 cm^{-1} are consistent with PEG absorbance, strongly suggesting the existence of PEG MWCNTs. The absorbance at 1730 cm^{-1} is typically associated with ester groups and indicates a chemical linkage between MWCNTs and PEG segments.

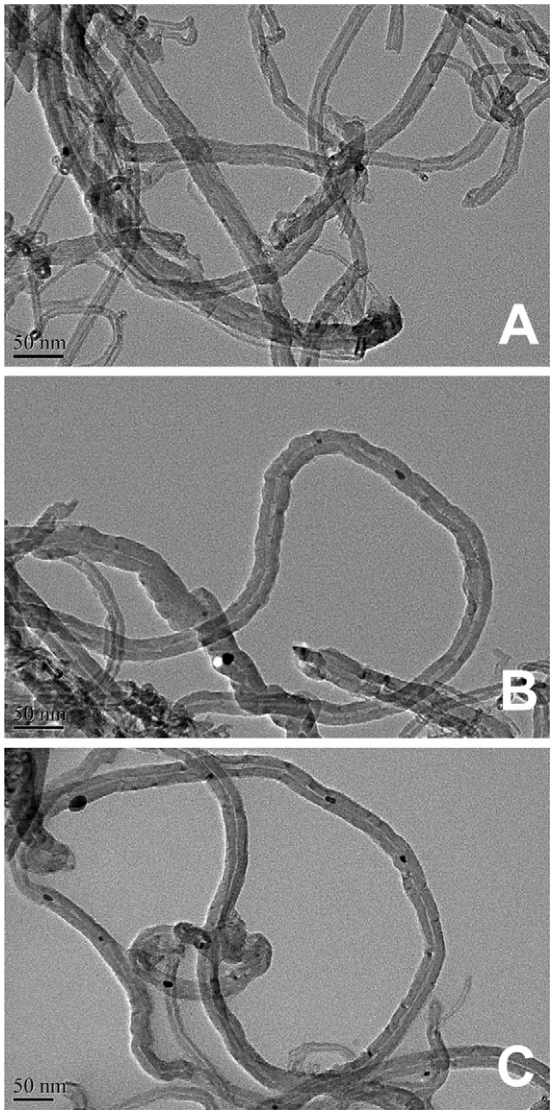

Fig. 2. Transmission electron microscopy image of pristine and functionalized MWCNTs. (A) Pristine MWCNTs; (B) MWCNTs-COOH; and (C) MWCNTs-PEG.

3.1.2. X-ray photoelectron spectroscopy (XPS)

The XPS of functionalized MWCNTs were recorded to confirm the linkage between MWCNTs and grafted groups (Fig. 1B). The scan of functionalized MWCNTs shows the presence of carbon and oxygen. Except for pristine MWCNTs, the COOH and PEG derivatives had an oxygen atom peak with a binding energy 532.5 eV [21].

3.1.3. Thermogravimetric analysis (TGA)

TGA is used to monitor how changes in manufacturing conditions affect the percentage of carbon nanotubes within a sample [22]. In the heating up to 500 °C, pristine MWCNTs lost about 1.3% of total weight (Fig. 1C). MWCNTs-PEG and MWCNTs-COOH lost 19.4% and 18.5% weight, respectively. Therefore, about 20 wt% of side groups were grafted onto MWCNTs, indicating the difference in properties between pristine and modified MWCNTs arose from these side moieties.

3.1.4. Transmission electron microscopy (TEM) images

TEM images reveal MWCNTs morphology (Fig. 2). The dispersibility and morphology of modified MWCNTs are similar but the pristine MWCNTs are slightly entangled. Although many recent studies report that MWCNTs toxicity is highly associated with morphological signatures, we do not think morphology in this experiment had a major impact on toxicological effects.

3.2. Cytotoxicity induced by MWCNTs

WST-8 data of MWCNTs, MWCNTs-COOH and MWNCTs-PEG indicated decreasing cytotoxicity in cell preparations incubated for 24 h (Fig. 3A). The results indicate that all MWCNTs at a concentration of 100 μg/mL significantly decreased the number of cells compared to untreated controls. However, only pristine MWCNTs impaired cell growth at 25 μg/mL. Loss of cell viability was apparently more pronounced with pristine MWCNTs compared to functionalized MWCNTs.

To further investigate potential cytotoxicity, RAW264.7 cells were exposed to MWCNTs and the amount of LDH released was evaluated. Exposure of MWCNTs (25–200 μg/mL) to RAW264.7 cells for 24 h resulted in significant ($p < 0.05$) changes in cell viability and lead to cell death (Fig. 3A), and LDH release into media in a concentration dependent manner (Fig. 3B), causing considerable membrane damage. Among the three MWCNTs, pristine MWCNTs produced a greater LDH release ($p < 0.05$) into the media compared to other concentrations above 100 μg/mL.

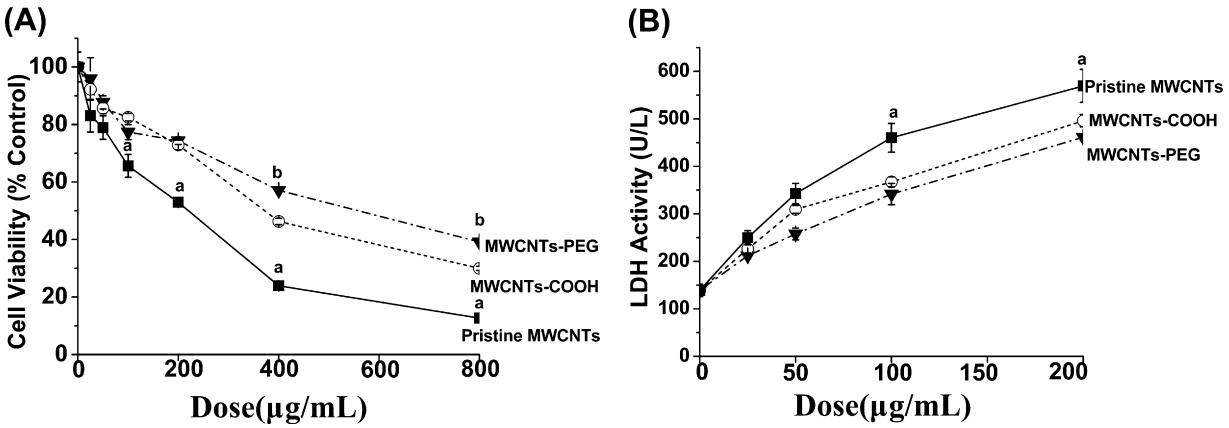

Fig. 3. Effects of three different MWCNTs samples on the cytotoxicity in RAW264.7 cells. (A) WST-8 assay results in cells treated with the different types of MWCNTs at 25–800 μg/mL concentrations for 24 h. (B) The concentration dependent membrane damage as determined by LDH leakage from RAW264.7 cells incubated with MWCNTs at 24 h. Data are the mean ± S.E.M. of three separate experiments. Significance was indicated by: [a] $p < 0.05$ *vs.* control cells. [b] $p < 0.05$ *vs.* pristine MWCNTs cells.

3.3. Inflammatory responses to MWCNTs

3.3.1. Expression and production of pro-inflammatory cytokines in RAW264.7 cells stimulated by MWCNTs

Since IL-1β, IL-6, and TNF-α are key mediators in inflammation and fibrosis [23], their expression level in macrophages following 24-h treatment with MWCNTs was investigated *via* real-time PCR (Fig. 4). Pristine MWCNTs did not cause a substantial increase in cytokine gene expression compared to functionalized MWCNTs. The negatively charged surface (MWCNTs-COOH) was more effective for induction of IL-1β, IL-6 and TNF-α than the neutral surfaces (MWCNTs-PEG). Impressively, these results are inconsistent with the effects of the MWCNTs on cell viability and membrane integrity. Judging from these data, the innate immune response of macrophages treated with MWCNTs suggests a dependency on surface functionality.

To evaluate the effect of MWCNTs on inflammatory cytokine production, IL-1β, IL-6, and TNF-α concentration in the culture medium was measured by ELISA. As Fig. 5 shows, exposure to MWCNTs-COOH produced a dose-dependent increase in IL-1β, IL-6, and TNF-α production for 24 h. No significant changes were observed in production of IL-1β and IL-6 for MWCNTs-PEG at concentrations ≥100 μg/mL, but TNF-α did exhibit a dose-dependent response. However, the production of IL-1β, IL-6, and TNF-α decreased in response to pristine MWCNTs at concentrations greater than 100 μg/mL (Fig. 5B and C). The progressive decrease in IL-1β, IL-6 and TNF-α production with increasing pristine MWCNTs concentrations was unexpected. This response may be due to a decrease in the number of live cells, which was observed in the cytotoxicity assays (Fig. 3). This response may be a manifestation of a latent form of nanotube cytotoxicity.

3.3.2. The induction of iNOS gene expression and NO release

Both iNOS gene expression and nitric oxide production were steadily increased in cell cultures stimulated with various doses of MWCNTs up to 24 h (Fig. 6). These results show that treatment with MWCNTs-COOH increased significantly both iNOS gene expression and nitric oxide production in a dose-dependent fashion ($p < 0.05$) (Fig. 6B). Furthermore, pristine MWCNTs stimulated RAW264.7 cells with respect to iNOS expression, and to a lesser extent, nitric oxide production ($p < 0.05$). In sharp contrast, there was neither iNOS expression nor nitric oxide production by RAW264.7 cells stimulated with MWCNTs-PEG ($p > 0.05$).

3.4. The dispersion and agglomeration state of MWCNTs

To provide a quantitative assessment, we used UV–VIS spectroscopy to assess time-dependent MWCNTs sedimentation. The hierarchical order of the suspension stability index in cell culture medium was MWCNTs-PEG > MWCNTs-COOH > pristine MWCNTs (Fig. 7). This demonstrated that the functionalization provided more stable dispersions than pristine MWCNTs. Significant agglomeration occurred in cells incubated with pristine MWCNTs. Pristine MWCNTs showed adherence to each other, forming dense micron-sized assemblies completely covering the cell surface (Fig. 8B). In contrast, MWCNTs-COOH and MWCNTs-PEG agglomerated slightly in medium and remained well dispersed after incubation (Fig. 8C and D). Particle behavior similar to that of MWCNTs-COOH was observed in preparations exposed to MWCNTs-PEG.

3.5. Cellular uptake of MWCNTs

3.5.1. Quantitative measurement of MWCNTs uptake by RAW264.7 cells

The standard turbidimetric method for determining MWCNTs concentration is a standard curve of absorbance *vs.* MWCNTs, which is used to determine amounts from the curve. The OD value was measured to quantify the amount of cell-associated MWCNTs. The time-course of changes in MWCNTs uptake by RAW264.7 cells exposed to 25 μg/mL MWCNTs is shown in Fig. 9. The cellular uptake of MWCNTs for the first 4 h was slow and reached 10% within 12 h.

3.5.2. TEM ultrastructure analysis on RAW264.7 cells treated by MWCNTs

To unambiguously demonstrate MWCNTs-uptake in RAW264.7 cells, we performed TEM analysis (Fig. 10). TEM micrographs show the presence of some small agglomerates of carbonaceous material as well as single nanotubes within treated cells. These images indicate that the cellular morphology was damaged and that the cells ingested a small amount of nanotubes. The nanotubes seem to be confined inside cells and distributed across the cytoplasm rather than in the nucleus. The nanoparticles appeared to be located in vesicles within the cytoplasm. Furthermore, the number of nanotubes per cell is related to the type of MWCNTs, and the amount of intercellular MWCNTs-COOH was larger compared to pristine MWCNTs (Fig. 10D).

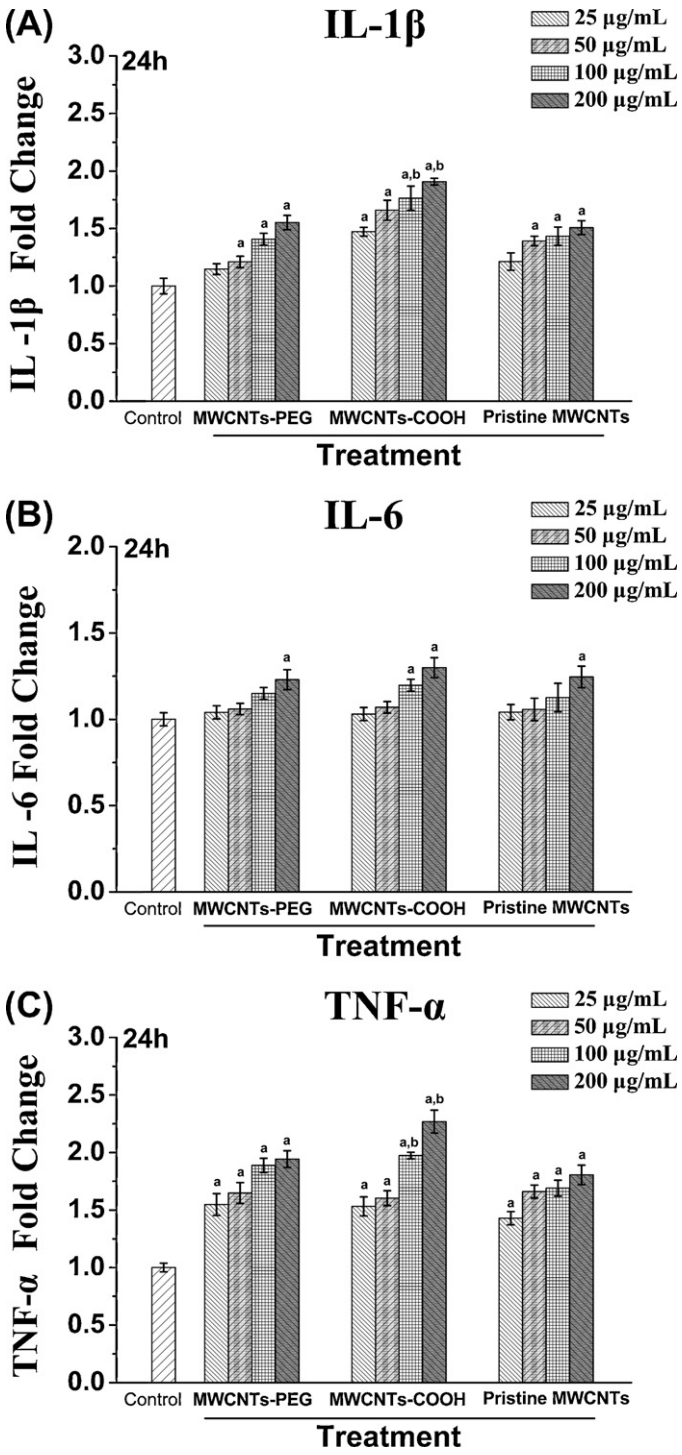

Fig. 4. qPCR analysis of mRNA expressions of (A) IL-1β, (B) IL-6 and (C) TNF-α in cells treated with the different types of MWCNTs at 25–200 μg/mL concentrations for 24 h. Data are the mean ± S.E.M. of three separate experiments. Significance was indicated by: [a] $p < 0.05$ *vs.* control cells. [b] $p < 0.05$ *vs.* pristine MWCNTs cells.

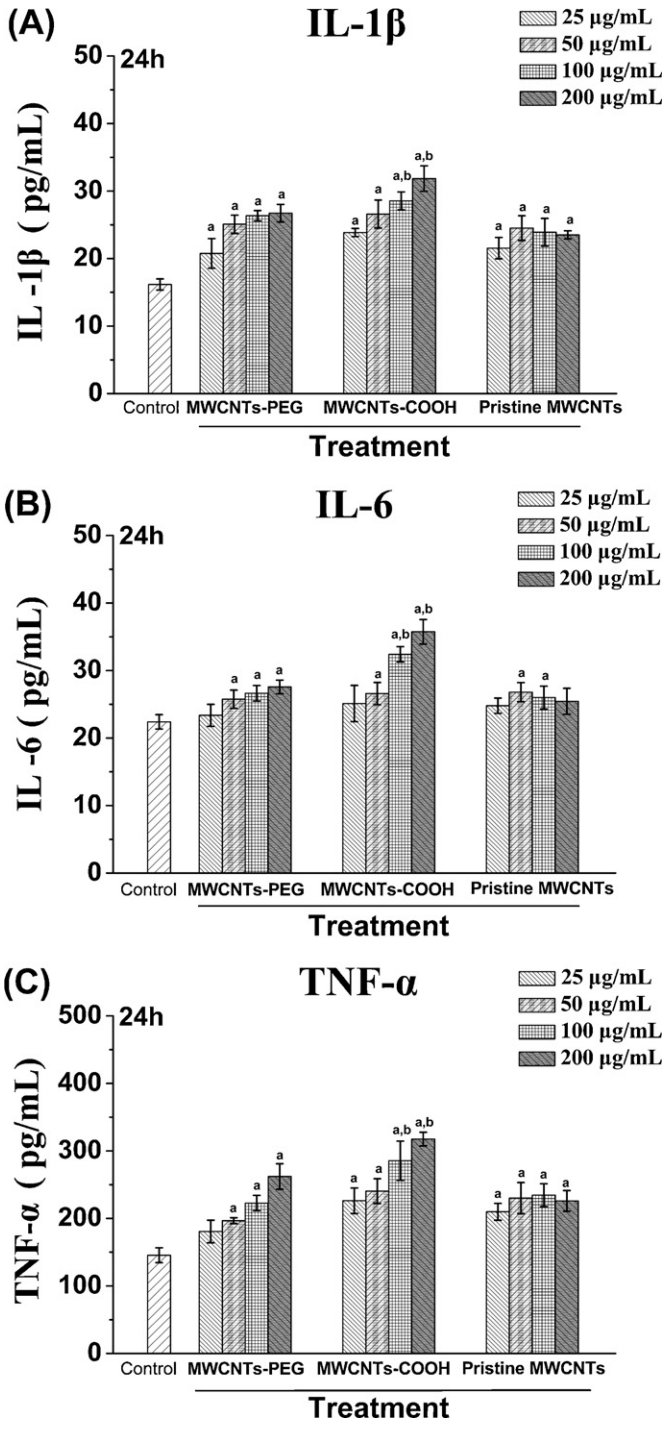

Fig. 5. Concentration-dependent pro-inflammatory cytokines production (A) IL-1β, (B) IL-6 and (C) TNF-α in RAW264.7 macrophages after incubation with the different types of MWCNTs at 25–200 μg/mL concentrations for 24 h. Data are the mean ± S.E.M. of three separate experiments. Significance was indicated by: [a] $p < 0.05$ *vs.* control cells. [b] $p < 0.05$ *vs.* pristine MWCNTs cells.

4. Discussion

We produced pristine and functionalized MWCNTs and characterized their cytotoxicity *in vitro*. Notably, pristine MWCNTs were more cytotoxic than MWCNTs-PEG and MWCNTs-COOH. Accordingly, the IC_{50} value of pristine MWCNTs was more than 1.5-fold that of the functionalized MWCNTs. We also noted that the highest LDH release was observed with pristine MWCNTs. These results indicate unmodified MWCNTs are highly cytotoxic in nature regardless of surface structure, probably because the cell membrane is easily injured by fibrous structures, and phagosomes or endosomes encompassing fibrous particles are fragile. It is also interesting to note the cytotoxic effects of MWCNTs depend on surface modifications. There are differences in cytotoxic effects of two functionalized MWCNTs: MWCNTs-COOH show more cytotoxicity than MWCNTs-PEG. The integrity of the cell monolayer may modulate cytotoxic effects of MWCNTs. We previously reported that the

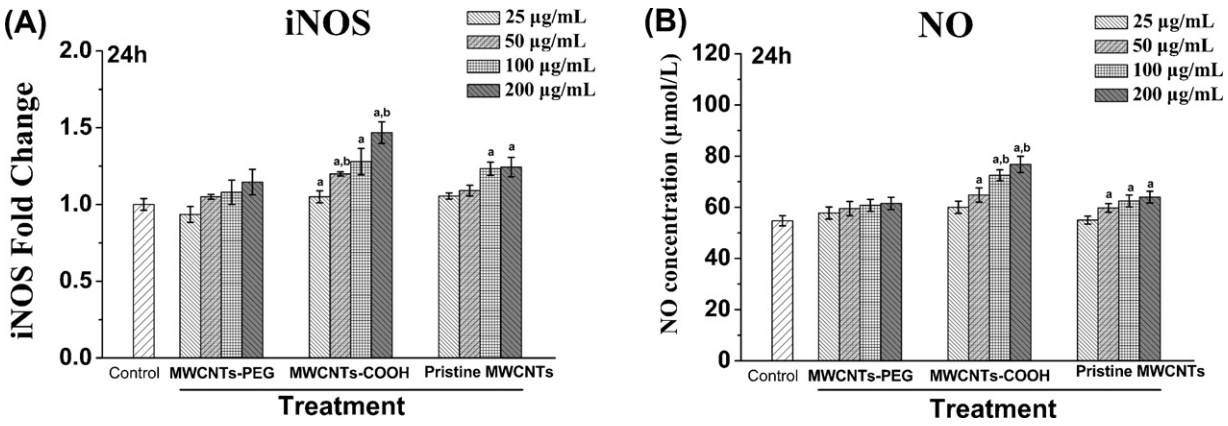

Fig. 6. The effect of MWCNTs on (A) iNOS mRNA expression and (B) nitrite production in cells treated with three types of MWCNTs at 25–200 μg/mL concentrations for 24 h. Data are the mean ± S.E.M. of three separate experiments. Significance was indicated by: $^{a}p < 0.05$ *vs.* control cells. $^{b}p < 0.05$ *vs.* pristine MWCNTs cells.

cell membrane of macrophages extended along MWCNTs, leading to membrane rupture [24].

Casals et al. [25] suggested that the biological activity and biokinetics of nanoparticles depend on different parameters: size, shape, chemistry, surface properties, agglomeration state, biopersistence, and dose. The influence of functionalization on CNTs toxicity is not clear, as divergent findings have been reported. A direct comparison of CNTs cytotoxicity results from different authors is difficult as results are highly dependent on concentration and specific CNTs characteristics [26]. Lacerda et al. [27] have reported that oxidation of CNTs allows for additional functionalization, which is associated with decreased cytotoxicity, as apparently these procedures help purify nanocarriers from catalytic metallic impurities (leading to improved biocompatibility). Moreover, some authors suggest functionalized CNTs contain lower levels of metallic impurities compared to pristine CNTs [10]. The present study shows that both pristine and functionalized MWCNTs induce cytotoxicity in RAW264.7 cells at concentrations higher than 25 μg/mL and 50 μg/mL, respectively. However, the content of Ni impurities in our nanotube samples (0.3–1.5 wt%) was much lower compared to Ni concentrations noted by previous studies [28,29] in SWCNTs (2.4–13.8 wt%, corresponding to a Ni dose of about 4 μg/mL in cell culture medium), which were unable to evoke cytotoxic effects. Similarly, the Fe content in the MWCNTs tested ranged between 0.05 and 0.25 wt% compared to the concentrations (0.08–4 wt%) found by Simon-Deckers et al. [29]. Therefore, it does appear that the presence of metal impurities in our MWCNTs samples is a primary toxicity factor.

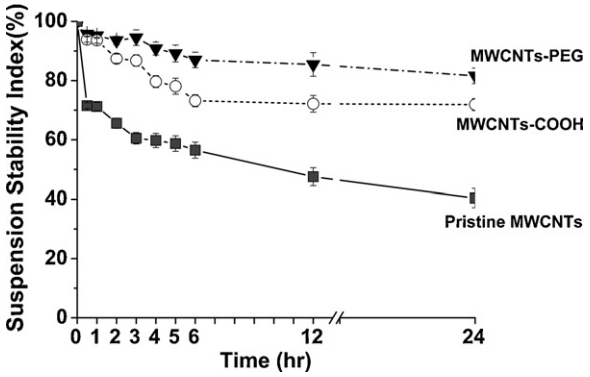

Fig. 7. Stability of pristine MWCNTs, MWCNTs-PEG, and MWCNTs-COOH suspensions in DMEM. The suspension stability index was calculated as the % of initial MWCNTs absorbance ($t = 0$) at $\lambda = 600$ nm for time periods of 1, 2, 3, 4, 5, 6, 12 and 24 h.

In addition to metal impurities, other factors such as solubility and agglomeration tendency can modify cytotoxic effects of CNTs. The precise impact of the agglomeration state on CNTs cytotoxicity remains to be clarified. In recent studies [30], MWCNTs with different degrees of agglomeration were investigated in D384 and A549 cells cultures, high dispersibility and low agglomeration tendency were relevant factors in modulating cytotoxicity. Cytotoxicity was more pronounced in cells exposed to highly agglomerated MWCNTs compared to better dispersed hf-MWCNTs-NH_2. Other experiments on the human mesothelioma cell line MSTO 211H, examined by MTT and cell proliferation assays, indicated stronger cytotoxic effects of agglomerated SWCNTs compared to well-dispersed nanotubes [28]. Under our experimental conditions, we used FBS as an agent to help suspend unfunctionalized multiwall nanotubes in culture medium. MWCNTs-PEG and MWCNTs-COOH were easily dispersible in medium with negligible tendency to form agglomerates. In addition, ultrasonication was used as the only procedure to improve dispersibility of the MWCNTs. As a result, more cytotoxicity was observed in cells exposed to highly agglomerated pristine MWCNTs compared to better dispersed functionalized MWCNTs.

Importantly, we measured the uptake of MWCNTs by RAW264.7 cells using a simple and high throughput method as described previously [20]. The time-course of MWCNTs uptake in RAW264.7 cells showed a sigmoidal curve. It probably took 1–2 h for most MWCNTs to deposit on the cell monolayer, and then the cells started to associate with MWCNTs for up to 12 h, at which time cell function had deteriorated because of exposure to MWCNTs.

Meanwhile, we also observed cellular uptake of MWCNTs by TEM. Several electron lucent voids (vacuoles) containing CNTs can be seen in the cytoplasm of the RAW264.7 cells. After 24 h incubation with RAW264.7 cells, the MWCNTs-COOH are internalized inside the cells, indicating that carboxyl groups are transporting CNTs inside cells effectively. This could be because MWCNTs-COOH have a hydrophilic surface coating with negatively charged –COOH, and their effects on protein adsorption have shown that fibronectin and albumin are more easily eluted from surfaces coated with –COOH [31]. The effect of cell adhesion peptides with –COOH functionality showed high levels of two fibronectin domains associated with structural and signaling components related to focal adhesions [32]. Favorable protein expression on the surface of –COOH functionalized nanoparticles may then lead to increased reactivity with cell membranes. A recent study has shown that –COOH functionalized surfaces enhance cellular uptake, and the amount of nanoparticle uptake could be correlated to the amount of –COOH functionality on the nanoparticle surface. Such interesting phenomena might be due to favorable interactions of the cell with the

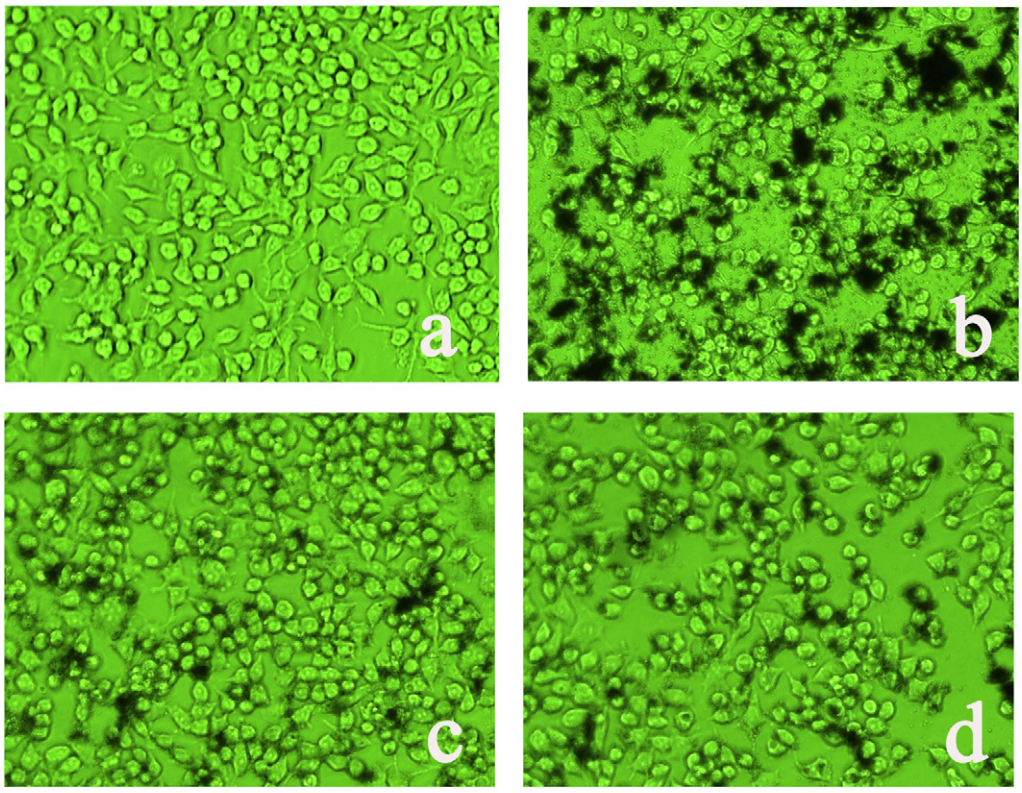

Fig. 8. Microscopy observation to show the dispersal of MWCNTs (100 μg/mL) in cell culture media. (A) Untreated cells; (B) MWCNTs: bundle-like agglomerates cover cell surface; (C) MWCNTs-COOH and (D) MWCNTs-PEG: slight agglomeration occurred with few black aggregates.

negatively charged coating [33]. These results suggest that cellular uptake of MWCNTs is positively correlated with their surface charge, and the negatively charged MWCNTs-COOH may facilitate transport of MWCNTs through the cell membrane. In contrast, we detected little MWCNTs-PEG located in the cellular interior after 24 h incubation, suggesting that MWCNTs-PEG in solutions were unable to traverse across cell membranes by themselves. PEGylation is known to reduce the interaction of particles with cells due to the formation of a hydrophilic stealth coating around the particles, leading to reduced uptake [34]. It is also known that hydrophilic PEG polymers can interfere with the formation of protein corona as well as particle opsonization, a mechanism in which opsonins play a key role in nanoparticle uptake in macrophages [35]. Similar findings have been reported for other PEG modified nanoparticles, such as quantum dots [36], and superparamagnetic magnetite nanoparticles [37].

In addition, a new translocation mechanism, called the "nanoneedle mechanism", was shown to be involved in cellular uptake of CNTs, where in CNTs acted as nanosized needles to pierce or penetrate membranes of many different cell types [38]. This hypothesis of the nanoneedle mechanism was theoretically demonstrated by molecular simulation [39]. However, further studies are needed to clarify the mechanisms for the differential cellular uptake of MWCNTs.

Evaluation of the pro-inflammatory response in macrophages treated with MWCNTs is important for nanotoxicological assessments. Cytokines play a key role in the pro-inflammatory response. Previous reports stated MWCNTs generated pro-inflammatory cytokines such as IL-6, IL-8, and MIF releases in BEAS-2B cells [20]. Iron-containing carbon nanotubes significantly stimulated TNF-α secretion in primary cultures of macrophages [40], and ammonium functionalized CNTs stimulated both TNF-α and IL-6 in primary cultures of peritoneal macrophages [41].

In our study, we were specifically interested in determining the effects of nanotubes at lower levels that were slightly cytotoxic. We found both MWCNTs-COOH and MWCNTs-PEG induced IL-1β expression under these conditions, which indicated stimulation could either be due to the functional groups or nanotubes and that the two effects could not be separated. In contrast, at the levels used, pristine MWCNTs did not induce IL-1β expression, which indicated they are not significantly stimulatory by themselves. The functionalized nanotubes were easily solubilized in water and all of them stimulated significant IL-6 and TNF-α expression. The most potent was the functionalized MWCNTs containing anionic and neutral

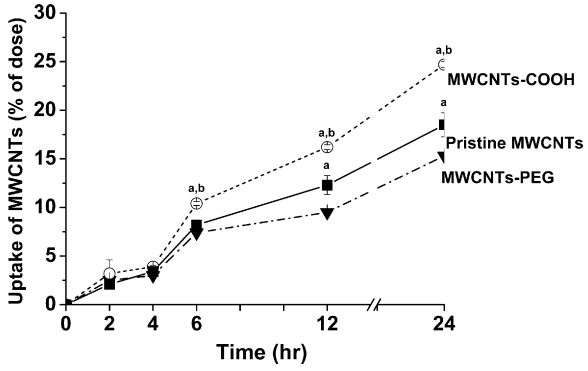

Fig. 9. Quantitative measurement of MWCNTs uptake by RAW264.7 cells. Cells were cultured in 6-well culture dishes to confluence and exposed to MWCNTs (25 μg/mL) up to 24 h. Dimethyl sulfoxide (0.2 mL) was added to each well and the lysate was pipetted thoroughly. A 250 μL sample was transferred to 96-well plates, and the OD (640 nm) was measured to quantify the amount of cell-associated MWCNTs. The value of cellular uptake was expressed as a percentage of total MWCNTs added to the well. Data are the mean ± S.E.M. of three wells. Significance was indicated by: $^{a}p < 0.05$ *vs.* control cells. $^{b}p < 0.05$ *vs.* pristine MWCNTs cells.

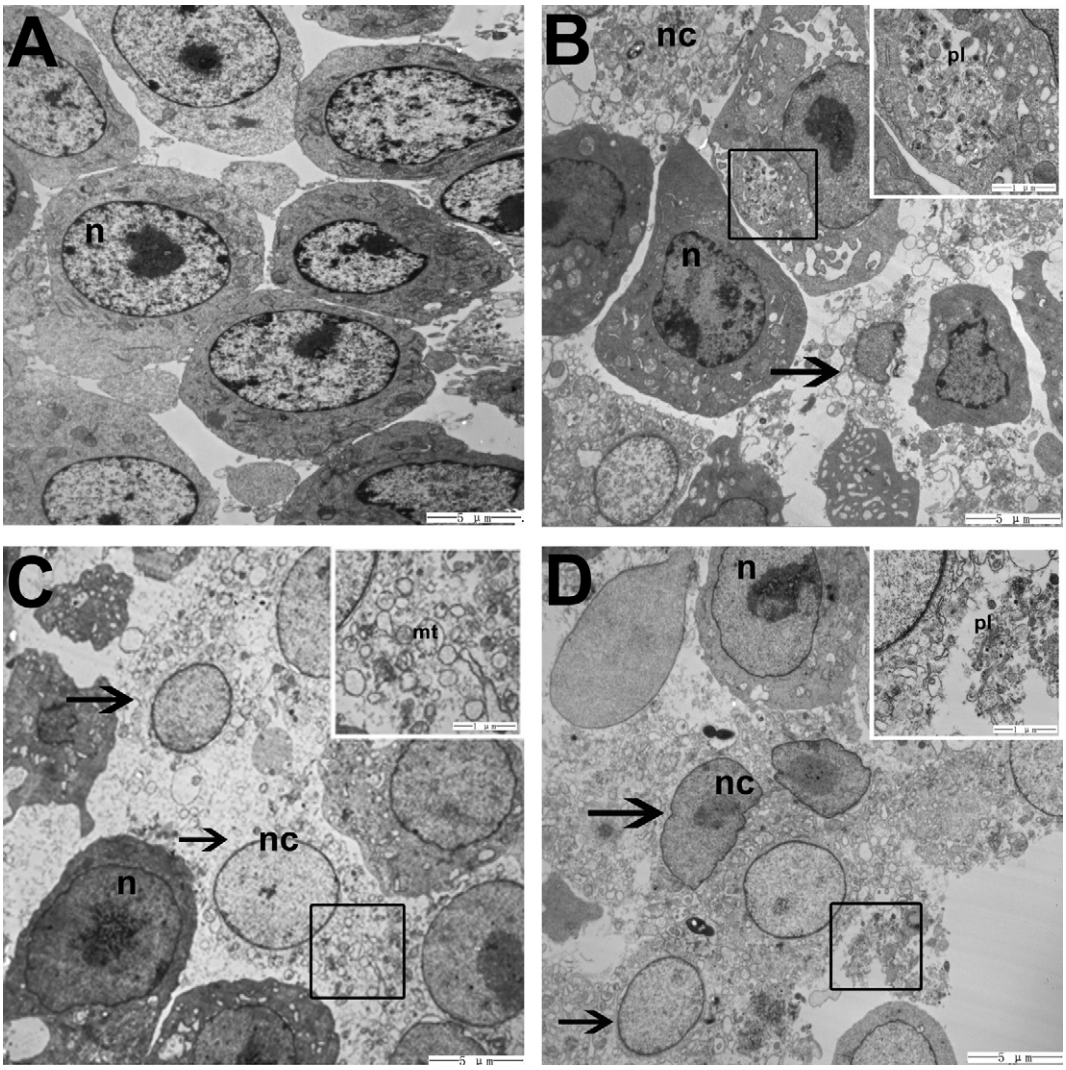

Fig. 10. TEM of RAW 264.7 cells treated with MWCNTs for 24 h; (A) micrograph of control, untreated cell; (B) pristine MWCNTs; (C) MWCNTs-PEG; and (D) MWCNTs-COOH. mt: mitochondrion; n: nucleus; nc: necrotic cell; pl: phagolysosome. Bar: 1 μm and 5 μm.

side groups. Furthermore, the functionalized nanotubes were more stimulatory than their non-functionalized counterparts.

While a number of studies have investigated MWCNTs and SWCNTs, fewer have looked specifically at the toxicity or biological effects of functionalized nanotubes. Functionalization of nanotubes that greatly increases their solubility in water and may allow them to enter cells. Non-functionalized nanotubes have been shown to damage macrophages and it is hypothesized that this may occur when the non-soluble nanotube binds to the cell membrane which is undergoing extension [24]. Given these observations, it may be necessary to draw more attention to the effects of functionalized nanotubes since many of the studies have used nanotubes with different functional groups.

5. Conclusions

Pristine and functionalized MWCNTs are able to interact with cells and induce different cytotoxic effects. Functionalization generated MWCNTs that exhibited mild to moderate cytotoxicity compared to pristine MWCNTs. However, functional groups are not equal in their effect and may cause an increase in inflammation. Physicochemical modifications of MWCNTs determine the state and stability of MWCNTs dispersions and cellular uptake, as well as their cytotoxic effects. In our opinion, it is vital to build up a complete array of tests, including thorough physicochemical characterization of nanotubes and the study of selected *in vitro* end-points such as oxidative stress, apoptosis, and inflammation.

Conflict of interest statement

The authors declare that there are no conflicts of interest.

Acknowledgments

This study was supported by Grants from the National Basic Research Program of China [2011CB933404], Doctoral Fund of Ministry of Education of China [20110092110041], National Natural Science Foundation of China [30972504 & 81172697], and Provincial Natural Science Foundation of Jiangsu [BK2011606].

References

[1] A.E. Porter, M. Gass, K. Muller, J.N. Skepper, P.A. Midgley, M. Welland, Direct imaging of single-walled carbon nanotubes in cells, Nat. Nanotechnol. 2 (2007) 713–717.
[2] A. Bianco, K. Kostarelos, M. Prato, Applications of carbon nanotubes in drug delivery, Curr. Opin. Chem. Biol. 9 (2005) 674–679.

[3] M. Bottini, S. Bruckner, K. Nika, N. Bottini, S. Bellucci, A. Magrini, A. Bergamaschi, T. Mustelin, Multi-walled carbon nanotubes induce T lymphocyte apoptosis, Toxicol. Lett. 160 (2006) 121–126.
[4] K. Donaldson, R. Aitken, L. Tran, V. Stone, R. Duffin, G. Forrest, A. Alexander, Carbon nanotubes: a review of their properties in relation to pulmonary toxicology and workplace safety, Toxicol. Sci. 92 (2006) 5–22.
[5] A.D. Maynard, R.J. Aitken, T. Butz, V. Colvin, K. Donaldson, G. Oberdorster, M.A. Philbert, J. Ryan, A. Seaton, V. Stone, S.S. Tinkle, L. Tran, N.J. Walker, D.B. Warheit, Safe handling of nanotechnology, Nature 444 (2006) 267–269.
[6] D. Cui, F. Tian, C.S. Ozkan, M. Wang, H. Gao, Effect of single wall carbon nanotubes on human HEK293 cells, Toxicol. Lett. 155 (2005) 73–85.
[7] L. Ding, J. Stilwell, T. Zhang, O. Elboudwarej, H. Jiang, J.P. Selegue, P.A. Cooke, J.W. Gray, F.F. Chen, Molecular characterization of the cytotoxic mechanism of multiwall carbon nanotubes and nano-onions on human skin fibroblast, Nano Lett. 5 (2005) 2448–2464.
[8] D.M. Brown, I.A. Kinloch, U. Bangert, A.H. Windle, D.M. Walter, G.S. Walker, C.A. Scotchford, K. Donaldson, V. Stone, An in vitro study of the potential of carbon nanotubes and nanofibres to induce inflammatory mediators and frustrated phagocytosis, Carbon 45 (2007) 1743–1756.
[9] R. Baktur, H. Patel, S. Kwon, Effect of exposure conditions on SWCNT-induced inflammatory response in human alveolar epithelial cells, Toxicol. In Vitro 25 (2011) 1153–1160.
[10] K. Pulskamp, S. Diabaté, H.F. Krug, Carbon nanotubes show no sign of acute toxicity but induce intracellular reactive oxygen species in dependence on contaminants, Toxicol. Lett. 168 (2007) 58–74.
[11] P.P. Simeonova, Update on carbon nanotube toxicity, Nanomedicine 4 (2009) 373–375.
[12] O. Vittorio, V. Raffa, A. Cuschieri, Influence of purity and surface oxidation on cytotoxicity of multiwalled carbon nanotubes with human neuroblastoma cells, Nanomedicine 5 (2009) 424–431.
[13] C.M. Sayes, F. Liang, J.L. Hudson, J. Mendez, W. Guo, J.M. Beach, V.C. Moore, C.D. Doyle, J.L. West, W.E. Billups, K.D. Ausman, V.L. Colvin, Functionalization density dependence of single-walled carbon nanotubes cytotoxicity in vitro, Toxicol. Lett. 161 (2006) 135–142.
[14] G. Jia, H. Wang, L. Yan, X. Wang, R. Pei, T. Yan, Y. Zhao, X. Guo, Cytotoxicity of carbon nanomaterials: single-wall nanotube, multi-wall nanotube, and fullerene, Environ. Sci. Technol. 39 (2005) 1378–1383.
[15] T. Zhang, M. Xu, L. He, K. Xi, M. Gu, Z. Jiang, Synthesis, characterization and cytotoxicity of phosphoryl choline-grafted water-soluble carbon nanotubes, Carbon 46 (2008) 1782–1791.
[16] M. Tim, Rapid colorimetric assay for cellular growth and survival: application to proliferation and cytotoxicity assays, J. Immunol. Methods 65 (1983) 55–63.
[17] T.D. Schmittgen, K.J. Livak, Analyzing real-time PCR data by the comparative C(T) method, Nat. Protoc. 3 (2008) 1101–1108.
[18] K.J. Livak, T.D. Schmittgen, Analysis of relative gene expression data using real-time quantitative PCR and the 2-[Delta][Delta]CT method, Methods 25 (2001) 402–408.
[19] X. Wang, T. Xia, S.A. Ntim, Z. Ji, S. George, H. Meng, H. Zhang, V. Castranova, S. Mitra, A.E. Nel, Quantitative techniques for assessing and controlling the dispersion and biological effects of multiwalled carbon nanotubes in mammalian tissue culture cells, ACS Nano 4 (2010) 7241–7252.
[20] S. Hirano, Y. Fujitani, A. Furuyama, S. Kanno, Uptake and cytotoxic effects of multi-walled carbon nanotubes in human bronchial epithelial cells, Toxicol. Appl. Pharmacol. 249 (2010) 8–15.
[21] C. Chen, B. Liang, A. Ogino, X. Wang, M. Nagatsu, Oxygen functionalization of multiwall carbon nanotubes by microwave-excited surface-wave plasma treatment, J. Phys. Chem. C 113 (2009) 7659–7665.
[22] P.X. Hou, S. Bai, Q.H. Yang, C. Liu, H.M. Cheng, Multi-step purification of carbon nanotubes, Carbon 40 (2002) 81–85.
[23] C.A. Feghali, T.M. Wright, Cytokines in acute and chronic inflammation, Front. Biosci. 2 (1997) 12–26.
[24] S. Hirano, S. Kanno, A. Furuyama, Multi-walled carbon nanotubes injure the plasma membrane of macrophages, Toxicol. Appl. Pharmacol. 232 (2008) 244–251.
[25] E. Casals, S. Vázquez-Campos, N.G. Bastús, V. Puntes, Distribution and potential toxicity of engineered inorganic nanoparticles and carbon nanostructures in biological systems, Trends Anal. Chem. 27 (2008) 672–683.
[26] D. Gutiérrez-Praena, S. Pichardo, E. Sánchez, A. Grilo, A.M. Cameán, A. Jos, Influence of carboxylic acid functionalization on the cytotoxic effects induced by single wall carbon nanotubes on human endothelial cells (HUVEC), Toxicol. In Vitro 25 (2011) 1883–1888.
[27] L. Lacerda, A. Bianco, M. Prato, K. Kostarelos, Carbon nanotubes as nanomedicines: from toxicology to pharmacology, Adv. Drug Deliv. Rev. 58 (2006) 1460–1470.
[28] P. Wick, P. Manser, L.K. Limbach, U. Dettlaff-Weglikowska, F. Krumeich, S. Roth, W.J. Stark, A. Bruinink, The degree and kind of agglomeration affect carbon nanotube cytotoxicity, Toxicol. Lett. 168 (2007) 121–131.
[29] A. Simon-Deckers, B. Gouget, M. Mayne-L'Hermite, N. Herlin-Boime, C. Reynaud, M. Carrière, In vitro investigation of oxide nanoparticle and carbon nanotube toxicity and intracellular accumulation in A549 human pneumocytes, Toxicology 253 (2008) 137–146.
[30] T. Coccini, E. Roda, D.A. Sarigiannis, P. Mustarelli, E. Quartarone, A. Profumo, L. Manzo, Effects of water-soluble functionalized multi-walled carbon nanotubes examined by different cytotoxicity methods in human astrocyte D384 and lung A549 cells, Toxicology 269 (2010) 41–53.
[31] C.D. Tidwell, S.I. Ertel, B.D. Ratner, B.J. Tarasevich, S. Atre, D.L. Allara, Endothelial cell growth and protein adsorption on terminally functionalized, self-assembled monolayers of alkanethiolates on gold, Langmuir 13 (1997) 3404–3413.
[32] S. Kannan, P. Kolhe, V. Raykova, M. Glibatec, R.M. Kannan, M. Lieh-Lai, D. Bassett, Dynamics of cellular entry and drug delivery by dendritic polymers into human lung epithelial carcinoma cells, J. Biomater. Sci. Polym. Ed. 15 (2004) 311–330.
[33] H. Verena, L. Myriam, W. Clemens Kilian, S. Hubert, L. Katharina, M. Volker, Synthesis and biomedical applications of functionalized fluorescent and magnetic dual reporter nanoparticles as obtained in the miniemulsion process, J. Phys. Condens. Matter 18 (2006) 2581–2594.
[34] M.R. Hamblin, J.L. Miller, I. Rizvi, H.G. Loew, T. Hasan, Pegylation of charged polymer-photosensitiser conjugates: effects on photodynamic efficacy, Br. J. Cancer 89 (2003) 937–943.
[35] D.E. Owens Iii, N.A. Peppas, Opsonization, biodistribution, and pharmacokinetics of polymeric nanoparticles, Int. J. Pharm. 307 (2006) 93–102.
[36] L.W. Zhang, N.A. Monteiro-Riviere, Mechanisms of quantum dot nanoparticle cellular uptake, Toxicol. Sci. 110 (2009) 138–155.
[37] Y. Zhang, N. Kohler, M. Zhang, Surface modification of superparamagnetic magnetite nanoparticles and their intracellular uptake, Biomaterials 23 (2002) 1553–1561.
[38] D. Pantarotto, J.P. Briand, M. Prato, A. Bianco, Translocation of bioactive peptides across cell membranes by carbon nanotubes, Chem. Commun. (Camb.) 7 (2004) 16–17.
[39] C.F. Lopez, S.O. Nielsen, P.B. Moore, M.L. Klein, Understanding nature's design for a nanosyringe, Proc. Natl. Acad. Sci. U. S. A. 101 (2004) 4431–4434.
[40] W.J. Waldman, R. Kristovich, D.A. Knight, P.K. Dutta, Inflammatory properties of iron-containing carbon nanoparticles, Chem. Res. Toxicol. 20 (2007) 1149–1154.
[41] H. Dumortier, S. Lacotte, G. Pastorin, R. Marega, W. Wu, D. Bonifazi, J.-P. Briand, M. Prato, S. Muller, A. Bianco, Functionalized carbon nanotubes are non-cytotoxic and preserve the functionality of primary immune cells, Nano Lett. 6 (2006) 1522–1528.